

# pH and SpO<sub>2</sub> Miniaturized Sensors for Fetal Health Monitoring

T. Nguyen<sup>1</sup><sup>a</sup>, A. Bessiere<sup>1</sup><sup>b</sup>, Q. Rousset<sup>2</sup><sup>c</sup>, B. Journet<sup>2</sup><sup>d</sup>, S. L'Horset<sup>2</sup><sup>e</sup>, H. Takhedmit<sup>1</sup>  
and G. Lissorgues<sup>1</sup><sup>f</sup>

<sup>1</sup>Université Gustave Eiffel, CNRS, ESYCOM UMR 9007, Noisy-le-Grand, France

<sup>2</sup>Lumin, ENS Paris Saclay, CentraleSupélec, Gif-sur-Yvette, France

**Keywords:** pH Sensor, SpO<sub>2</sub> Sensor, Micro-Electrodes.

**Abstract:** In this paper we present a prototype which is a first attempt to get continuous fetal health monitoring during labor. This system is capable of simultaneously measuring pH, SpO<sub>2</sub> and provides a clear photoplethysmogram in real time. A Titanium nitride pH sensing electrode of 600 μm diameter in size performed a linear Nernstian sensitivity of 62.8 mV/pH within the pH range of interest from 6 to 8 and a precision of 0.14 in pH. The reflectance SpO<sub>2</sub> sensor employed two LEDs at 630 nm and 940 nm wavelengths and is monitored by a MSP432 microcontroller; the result recorded shows close behavior to a commercial device. This work is under optimization process for a better accuracy and aiming for integration into a specific miniaturized device with a touch screen as user interface.


## 1 INTRODUCTION


Monitoring fetal well-being during labor is a common practice of daily obstetrical activities. Ensuring the good oxygenation of the fetus is important to prevent the risk of asphyxiation and its most serious consequences: peripartum death and distant sequelae, in particular neurological disorders including psychomotor disability or cerebral palsy (Carbonne & Nguyen, 2008). Capillary pH on fetal scalp is frequently monitored as a second-line examination beside fetal heart rate in delivery rooms, to reduce false positives rate for predicting the fetal acidosis. The technique of collecting capillary samples from fetal scalp has many limitations in terms of discontinuity and high rate of failures. Indeed, taking a discontinuous sample every 30 minutes appears obsolete in some obstetrical situations.


It was demonstrated that the correlation between tissue pH and capillary pH at birth is good (Weber, 1980). Several teams have developed continuous measurement systems for tissue pH at the fetal scalp,


using miniaturized glass electrode (Stamm et al., 1976), optical fiber and pH indicator colorimetric (Peterson et al., 1980). However, the methodologies set out in these publications were stagnant because of the technical limitations at the time, mainly related to the fabrication techniques and miniaturization issues not available in the 1980s.


Potentiometric based pH sensors are the most favored electrochemical systems due to their simple design and possibility to be miniaturized (Kurzweil, 2009). A potentiometric based sensor includes one working electrode (WE) and one reference electrode (RE). In principle, when the sensor is immersed in the test solutions, a potential difference between the WE and the RE (open circuit voltage) is produced and proportional to the pH variation. The most common material of RE is Ag/AgCl, due to its stable potential. Some pH-sensitive materials have been reported including metal oxides such as Iridium(IV) oxide (IrO<sub>2</sub>), Ruthenium(IV) oxide (RuO<sub>2</sub>), Tungsten trioxide (WO<sub>3</sub>) and Titanium dioxide (TiO<sub>2</sub>) etc., conductive polymers such as poly-aniline, polypyrrole, etc., and typically, the glass pH electrode


<sup>a</sup> <https://orcid.org/0000-0002-2355-487X>

<sup>b</sup> <https://orcid.org/0000-0003-0304-4538>

<sup>c</sup> <https://orcid.org/0000-0001-8468-8487>

<sup>d</sup> <https://orcid.org/0000-0001-7278-7170>

<sup>e</sup> <https://orcid.org/0000-0001-7308-0900>

<sup>f</sup> <https://orcid.org/0000-0003-3371-8353>

with an ideal Nernstian sensitivity. However, these devices still have some drawbacks in terms of potential drift and selectivity (metal oxides), stability and long-term storage (polymers), fragility and improbability of biomedical application (glass electrode) (Manjakkal et al., 2020).

To the best of our knowledge, Titanium nitride (TiN) is the only metal nitride reported for potentiometric pH sensors, and is considered as an alternative pH-sensing material. Thin TiN films have been reported to reach 0.01 pH precision which is critical for the fetal scalp tissue pH measurements (Paul Shylendra et al., 2020). Therefore, the first part of our work focuses on developing a TiN potentiometric pH micro-sensor.

In this study, we attempt to design a prototype for the first time to continuously monitor fetal tissue pH during labor, combined with fetal oxygen saturation ( $\text{SpO}_2$ ) as control. A microelectrode of 600  $\mu\text{m}$  diameter was fabricated using Titanium nitride (TiN) as the potentiometric sensing material for pH variations. An optical sensor made of two LEDs and one photodiode was used for  $\text{SpO}_2$  monitoring, based on the absorption spectra of the oxygenated and deoxygenated hemoglobins. The signal waveform also known as photoplethysmogram (PPG) can be useful to determine pulse wave characteristics, such as dicrotic notch, systolic and diastolic phases. The data acquired from these sensors including pH,  $\text{SpO}_2$ , heart rate and PPG can be saved in a SD card and be displayed on a LCD touchscreen.

## 2 DESIGN AND FABRICATION

### 2.1 pH Sensor Fabrication and Characterization Procedure

Electrodes of 600  $\mu\text{m}$  diameter in size were fabricated following this process: (1) a gold/titanium tungsten (Au/TiW) layer of 520 nm in thickness was deposited on a glass substrate (Alcatel sputtering), (2) a positive photoresist was spin coated on top of the gold layer for ultraviolet photolithography, development and etching, (3) the photoresist was removed, (4) the process was repeated with the second which is then TiN of 200 nm thick (Plassys sputtering) and (5) completed with the third layer of 1.7  $\mu\text{m}$  thick photoresist SU8 used as an insulator with the openings on the electrode and contact pad areas. Figure 1 illustrates the design of the electrode with the corresponding microscope image on Figure 2.

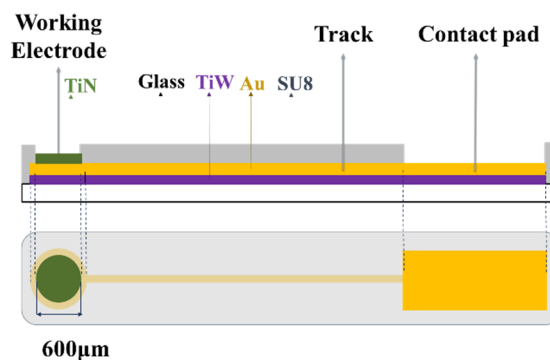


Figure 1: pH sensing electrode design with three layers TiW/Au, TiN and SU8 on a glass substrate, top/cut view, bottom/top view.

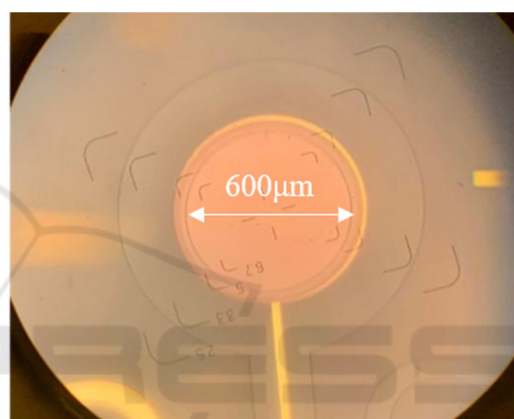


Figure 2: Image of the fabricated pH sensing electrode under microscope.

The fabricated electrodes were equilibrated in deionized water overnight before characterization to obtain stable potential.

The potentiostat SP-200 from Biologic Science Instrument was used to carry out electrochemical measurements. An Ag/AgCl electrode was used as the RE. Open circuit voltage (OCV) or open circuit potential was measured in phosphate-buffered saline (PBS) test solutions with pH ranging from 6 to 8 at 25°C, with 0.2 pH step to determine sensitivity, stability, response time, hysteresis and reproducibility of the pH sensor. The WE and the RE were submerged sequentially in the test solutions disregarding cross-contamination. A commercial glass electrode from Atlas Scientific was used to confirm the pH level of the solution under testing.

## 2.2 SpO<sub>2</sub> Sensor Scheme and PCB Design

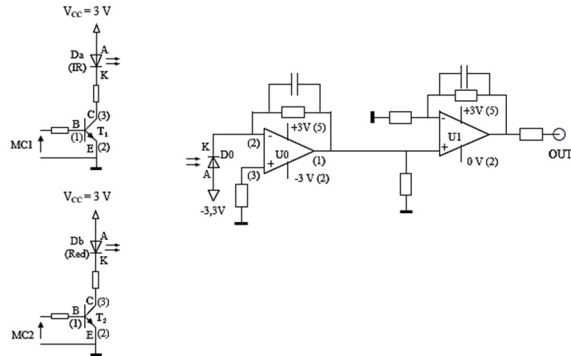


Figure 3: Scheme of the optical reflectance SpO<sub>2</sub> sensor. The circuit consists of two LEDs of 630 nm (Red) and 940 nm (IR) wavelength, one photodiode (D0), switching signals from microcontroller MSP432 (MC1 and MC2 inputs), transistors MMBT3904 (T1 and T2) and two operational amplifiers OPA376 (U0 and U1).

Figure 3 shows the scheme of the SpO<sub>2</sub> sensor. The circuit consists of two LEDs of 630 nm (Red, LS L29K) and 940 nm (IR, KP-2012F3C) wavelengths. The light transmitted through the skin is detected by a PIN photodiode (BP 104 S). On the sensing board a transimpedance amplifier stage and a second operational amplifier stage, both based on operational amplifier OPA376, are used to amplify the signal and to drive the cable connected to the microcontroller board.

This sensor is fabricated on a classical FR4 Printed Circuit Boards (PCB) and will be later implemented on a Polyimide flexible substrate (Figure 4). MSP432 is used to control the LEDs, to achieve the data sampling by a 14 bits Analog to Digital Converters (ADC) and to perform some signal processing. A band pass filter with 5 Hz high cutoff frequency and 1 Hz low cutoff frequency is implemented to obtain clear PPG signals.

The LEDs are activated sequentially from pulses delivered by the microcontroller at a frequency of 200 Hz, the pulse width is 220 μs. Sampling is done in the middle of a pulse. The LEDs information is acquired and separated in the microcontroller leading to two digitized signals for each one. The corresponding peak-to-peak amplitudes (AC for Alternating Current) and mean values (DC for Direct Current) are determined to calculate a ratio (R) value as given by equation 1. As until now we did not make the complete calibration, the SpO<sub>2</sub> is determined using the R value and an empirical formula (equation 2), based on application note AN1525 from Zhang Feng, Microchip Technology.

$$R = \frac{AC^{red}/DC^{red}}{AC^{IR}/DC^{IR}} \quad (1)$$

$$SpO_2 = 119 - 32.5R \quad (2)$$

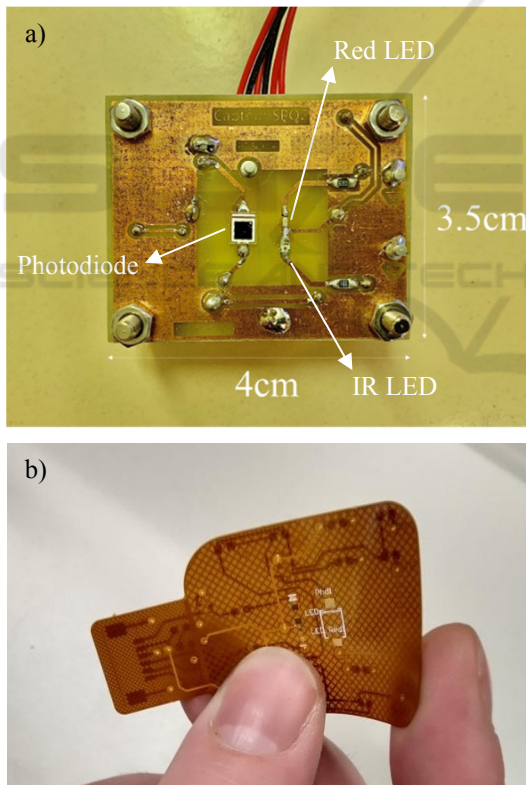


Figure 4: a) SpO<sub>2</sub> sensing board composed of a Red LED (630 nm), an IR LED (940 nm), a photodiode, a transimpedance amplifier and a second amplifier stage. b) The flexible printed circuit board (PCB) made in Polyimide, without components, for next step integration.

## 3 RESULTS AND DISCUSSION

### 3.1 TiN Electrode Characterization for pH Sensing Application

The sensitivity of the TiN electrodes fabricated with the above described clean room process as a potentiometric sensor was determined by measuring the OCV values at different pH levels of the test solutions during 100 s. The recorded data from 50 s to 100 s were averaged to calculate the sensitivity of TiN electrode as shown in Figure 5. The slope of the curve is 62.8 mV/pH corresponding to the sensitivity

Table 1: Potentiometric pH sensor performance of different materials.

Material	Sensitivity (mV/pH)	Response time (s)	Reference
TiN NP	46.48	5.2	(Liu et al., 2016)
TiN NTA	55.33	4.4	(Liu et al., 2016)
TiN thin film	57.5	-	(Paul Shylendra et al., 2020)
IrO <sub>2</sub>	69.9 ± 2.2	0.5 s	(Chung et al., 2014)
IrO <sub>2</sub>	51	0.9 to 2 s	(Huang et al., 2011)
Polyaniline	58 ± 0.3	20	(Guinovart et al., 2014)
Polyaniline	62.4	12.8	(Park et al., 2019)
Polyaniline/Zeolite blend	310 ± 40	-	(Malkaj et al., 2006)
Polypyrrole/Zeolite blend	1300 ± 100	-	(Malkaj et al., 2006)

of the TiN electrode. The correlation coefficient was calculated to be 0.998 and the standard reduction potential E is 402.6 mV, corresponding to the intercept of the curve.

This sensitivity is higher than the reported results of sputtered TiN film with the same thickness of TiN layer (57.5 mV/pH, R<sup>2</sup> = 0.9999), (Paul Shylendra et al., 2020), TiN nanotube array (TiN NTA, 55.33 mV/pH, R<sup>2</sup> = 0.995), and TiN nano powder (TiN NP, 46.48 mV/pH, R<sup>2</sup> = 0.992), (Liu et al., 2016).

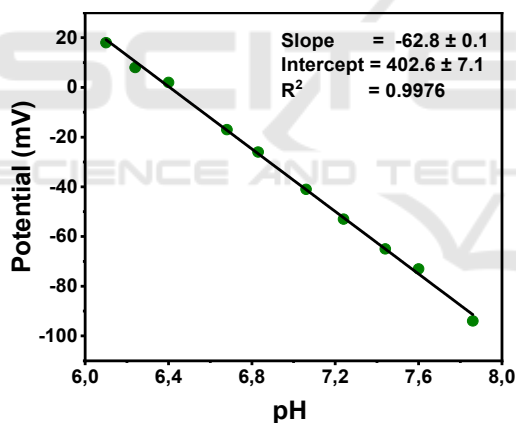


Figure 5: OCV curve and sensitivity of our fabricated TiN electrode.

Data from Table 1 show that we should achieve a better sensitivity than most of the other materials. Especially compared to IrO<sub>2</sub>, which has been developed for in-vivo and in-vitro applications, our TiN electrode has shown a comparable sensitivity. It was however reported a greater sensitivity in conductive polymer - based sensors such as polyaniline and polypyrrole blends (310 ± 40 mV/pH and 1300 ± 100 mV/pH, respectively) (Korostynska et al., 2008). Yet, their application is still limited due its tendency to become unstable over time.

The response time of the TiN electrode was measured by immersing the WE and the RE continuously in PBS solutions with pH levels from 6.10 to pH 7.74. The time for the signal to reach 90 % of equilibrium value is 10 s (Figure 6), which is comparable and even better than some reported polymer-based potentiometric pH sensors (Table 1). This response time is slower than that of TiN NTA (4.4 s), TiN NP (5.2 s) (Liu et al., 2016) and IrO<sub>2</sub> (0.5 s to 2s) (Manjakkal et al., 2020). This can be explained by the low porosity of the surface of our TiN layer (ability to trap more ions in a certain area), which is expected to be improved in the next fabrication process after a specific surface treatment.

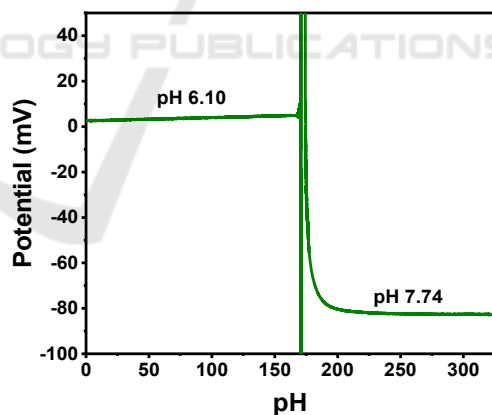


Figure 6: The response time of TiN in PBS. The parasite signal in between two pH levels is only due to manipulation during the experiment.

Figure 7 shows the stability of the open circuit potential of the same electrode in different pH levels during 200 s. A potential drift of less than 3 mV was observed during the first 50 s but stabilized after that. This drift might have been caused by the hydrogen ion trapping and diffusion phenomena into the lattice of the material.



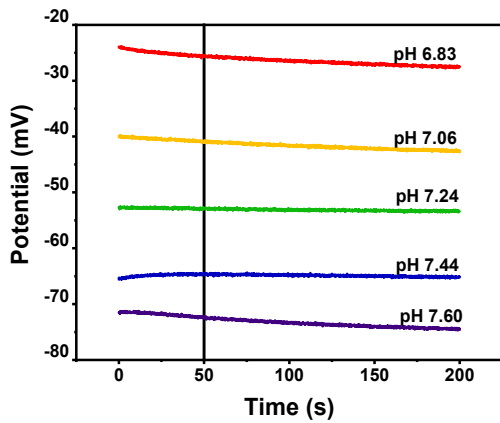


Figure 7: The stability of one TiN electrode at different pH levels of PBS solutions during 200 s.

A hysteresis of 10 mV was observed with the pH range from 6 to 7.6 during 6 cycles, as shown in Figure 8. The hysteresis could be caused by the cross-contamination and possibly by condition differences in the testing process, such as the stability of pH test solutions, temperature and connection problems. Since we are looking at a small variation of pH in a narrow clinical-related pH range, the experiment still needs to be improved to evaluate accurately the performance of the electrode including operation at 37°C.

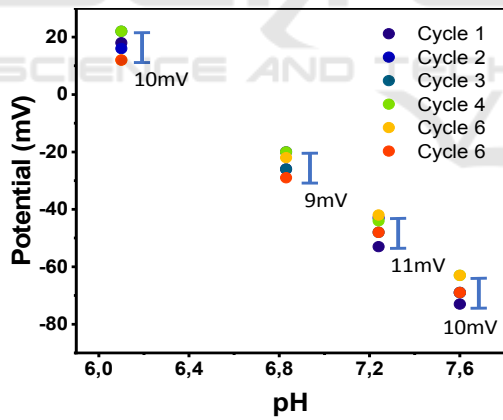


Figure 8: OCV of one TiN electrode during 6 cycles.

Reproducibility during 3 loops of measurements on the same electrode is presented in Figure 9. The variation of the pH value was calculated to be 0.14 (by hysteresis over sensitivity), which represented the precision of our electrode. It is not yet sufficient for the fetal tissue pH monitoring application but already interesting for other applications. The optimization is undergoing by varying the TiN fabrication parameters, changing its surface properties

(roughness) to improve the performance of the TiN electrodes.

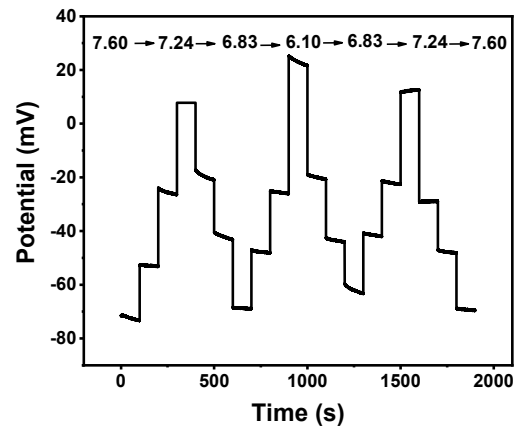


Figure 9: The reproducibility of one TiN electrode during 3 loops measurements in 4 pH levels: 6.10, 6.83, 7,24, 7.60.

### 3.2 SpO<sub>2</sub> Measurement as Control for Fetal Monitoring

We present here the characterisation of our SpO<sub>2</sub> circuit described in Figure 3. We need to develop our own chip for later integration of both pH and SpO<sub>2</sub> sensors in a unique miniaturized device adapted to the fetal head positioning.

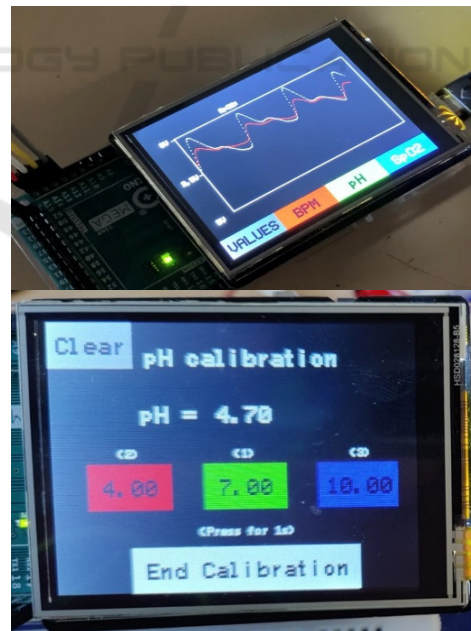


Figure 10: A touchscreen (2.8") to display in real time the signals (choice between pH or SPO<sub>2</sub>), integrated to a SD card to save data as simple user interface.

Figure 10 shows a simple user interface based on a touch screen display and Figure 11 shows a comparison between the raw data collected from the sensing board and the filtered data for display purposes and easy readings. The noise, including 50 Hz, is significantly reduced to obtain clear waveforms.

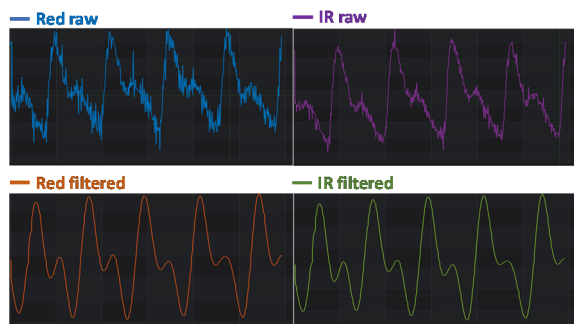


Figure 11: Comparison between raw signals sent from the sensing board and the filtered signals by a band-pass filter with 5 Hz high cutoff frequency and 1 Hz low cutoff frequency.

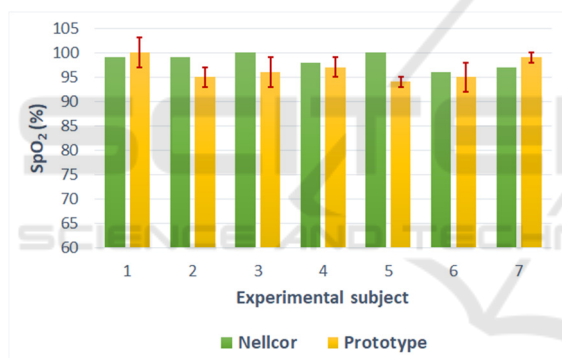


Figure 12: Comparison between the SpO<sub>2</sub> measured by Nellcor device (green) and our prototype (yellow) on the middle finger of seven healthy individuals. The error bars are in absolute values.

A commercial Nellcor pulse oximeter was used for a comparison with the SpO<sub>2</sub> prototype. We have done measurements with both tools simultaneously on the middle finger of seven healthy individuals. In each measurement by the prototype, we waited at least one minute before recording data to be sure that the signal was stabilized. We accessed the results by comparing the average values in 2 minute intervals. The errors of measured signal by the prototype varied from 1 to 6% in absolute values, as seen on Figure 12. The average relative error of the prototype compared to the Nellcor device is -1,9%. The difference between the two mean values comes from the use of equation 2 for a non-calibrated device. Some

influencing factors have been observed, which are the pressure of the finger to the sensing board, the skin color, the perspiration and the difference in thickness of epidermis. This should be overcome by improving the mechanical design and packaging of the sensor. However, the behaviour of the prototype is quite close to the reference system from Nellcor.

## 4 CONCLUSIONS

A prototype capable of measuring simultaneously pH and SpO<sub>2</sub> has been developed showing promising initial performance. At this stage, the sensors are separated but an integrated package is considered for the next step using a flexible electronic circuit for SpO<sub>2</sub> and flexible substrate fabrication for the pH sensor.

A 600 μm diameter pH sensing electrode that was constructed from Titanium nitride (TiN), performed a linear Nernstian sensitivity of 62.8 mV/pH within the pH range from 6 to 8 and a precision of 0.14. This pH sensing electrode is under optimization targeting fetal tissue pH monitoring application.

The optical reflectance SpO<sub>2</sub> sensor was designed, a microcontroller MSP432 being employed to control the light emission and data acquisition at 200 Hz frequency. Our SpO<sub>2</sub> sensor produced a quite close behavior to commercial devices and a clear PPG signal available through a customized simple interface. This work is under the optimization stage and is expected to be embedded with all above-mentioned sensors into a flexible solution for later in vivo testing.

Indeed, as stated in the introduction, capillary pH on fetal scalp is frequently monitored as a second-line examination beside fetal heart rate in delivery rooms, to reduce false positives rate for predicting the fetal acidosis. Our project is to integrate on a unique device both SpO<sub>2</sub> and pH sensors with a continuous monitoring.

In the final form of the device, the flexible pH electrodes could be considered to be attached into a specific needle, which is adaptable for clinical skin insertion. This pH sensing needle will be fixed with the SpO<sub>2</sub> sensing board using a flexible polyimide substrate in a customized design package.

The important challenges to be considered for this work are: 1) to find the best mechanical design to be easily used by the medical staffs and prevent any damage for the foetus and the mother; 2) to guarantee the sensitivity in real use-case and 3) to establish a protocol for sterilization and storage of the pH sensing electrodes and the SpO<sub>2</sub> sensor.

## ACKNOWLEDGEMENTS

We express our gratitude to L. Rousseau, C. Wilfinger and U.T. Sarah for their support on TiN fabrication in ESIEE PARIS clean room and Prof. E. Lecarpentier at intercommunal hospital center in Créteil (CHIC) for his advice on medical application issues.

## REFERENCES

- Carbonne, B., & Nguyen, A. (2008). Surveillance fœtale par mesure du pH et des lactates au scalp au cours du travail. *Journal de Gynécologie Obstétrique et Biologie de la Reproduction*, 37(1), S65–S71.
- Chung, H.-J., Sulkin, M. S., Kim, J.-S., Goudeseune, C., Chao, H.-Y., Song, J. W., Yang, S. Y., Hsu, Y.-Y., Ghaffari, R., Efimov, I. R., & Rogers, J. A. (2014). Stretchable, Multiplexed pH Sensors With Demonstrations on Rabbit and Human Hearts Undergoing Ischemia. *Advanced Healthcare Materials*, 3(1), 59–68.
- Guinovart, T., Valdés-Ramírez, G., Windmiller, J. R., Andrade, F. J., & Wang, J. (2014). Bandage-Based Wearable Potentiometric Sensor for Monitoring Wound pH. *Electroanalysis*, 26(6), 1345–1353.
- Huang, W.-D., Cao, H., Deb, S., Chiao, M., & Chiao, J. C. (2011). A flexible pH sensor based on the iridium oxide sensing film. *Sensors and Actuators A: Physical*, 169(1), 1–11.
- Korostynska, O., Arshak, K., Gill, E., & Arshak, A. (2008). Review Paper: Materials and Techniques for *In Vivo* pH Monitoring. *IEEE Sensors Journal*, 8(1), 20–28.
- Kurzweil, P. (2009). Metal Oxides and Ion-Exchanging Surfaces as pH Sensors in Liquids: State-of-the-Art and Outlook. *Sensors*, 9(6), 4955–4985.
- Liu, M., Ma, Y., Su, L., Chou, K.-C., & Hou, X. (2016). A titanium nitride nanotube array for potentiometric sensing of pH. *The Analyst*, 141(5), 1693–1699.
- Malkaj, P., Dalas, E., Vitoratos, E., & Sakkopoulos, S. (2006). PH electrodes constructed from polyaniline/zeolite and polypyrrole/zeolite conductive blends. *Journal of Applied Polymer Science*, 101(3), 1853–1856.
- Manjakkal, L., Dervin, S., & Dahiya, R. (2020). Flexible potentiometric pH sensors for wearable systems. *RSC Advances*, 10(15), 8594–8617.
- Park, H. J., Yoon, J. H., Lee, K. G., & Choi, B. G. (2019). Potentiometric performance of flexible pH sensor based on polyaniline nanofiber arrays. *Nano Convergence*, 6(1), 9.
- Paul Shylendra, S., Lonsdale, W., Wajrak, M., Nur-E-Alam, M., & Alameh, K. (2020). Titanium Nitride Thin Film Based Low-Redox-Interference Potentiometric pH Sensing Electrodes. *Sensors*, 21(1), 42.
- Peterson, J. I., Goldstein, S. R., Fitzgerald, R. V., & Buckhold, D. K. (1980). Fiber optic pH probe for physiological use. *Analytical Chemistry*, 52(6), 864–869.
- Stamm, O., Latscha, U., Janecek, P., & Campana, A. (1976). Development of a special electrode for continuous subcutaneous pH measurement in the infant scalp. *American Journal of Obstetrics and Gynecology*, 124(2), 193–195.
- Weber, T. (1980). Continuous Fetal Scalp Tissue pH Monitoring During Labor: An Analysis of 152 Consecutive Cases. *Acta Obstetrica et Gynecologica Scandinavica*, 59(3), 217–223.